Chimeric Antigen Receptor T-Cell Recruitment and Killing can be Evaluated on an Organ-Chip Model System

Anita K. Mehta[1], Irene Jacob[1], Isaac Downs[1], Marianne Kanellias[1], Adriana V. Cespedes[1], Anthony R. Heng[1], Lorna Ewart[1]

[1] Emulate, Inc., 27 Drydock Avenue, Boston, MA, 02210, USA

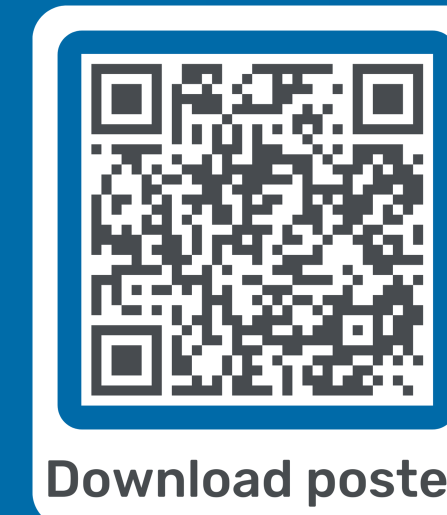

Objective:

Chimeric antigen receptor (CAR) T-cell therapy holds great promise for treating solid tumors. However, there are significant challenges in developing an effective CAR T cell solid tumor therapy due to a lack of human-relevant models that adequately capture mechanisms of CAR T cell recruitment– a critical rate-limiting step in CAR T cell efficacy that is often overlooked. Here, we have developed a novel system for investigating both the recruitment and killing capacity of CAR T cells in an Organ-Chip model.

Modeling Workflow for Solid Tumor CAR T-cell Therapy Evaluation

1. Top Channel
2. Tumor Cell Line
3. Vacuum Channel
4. Porous Membrane
5. CAR T Cells
6. Endothelial Cells
7. Bottom Channel

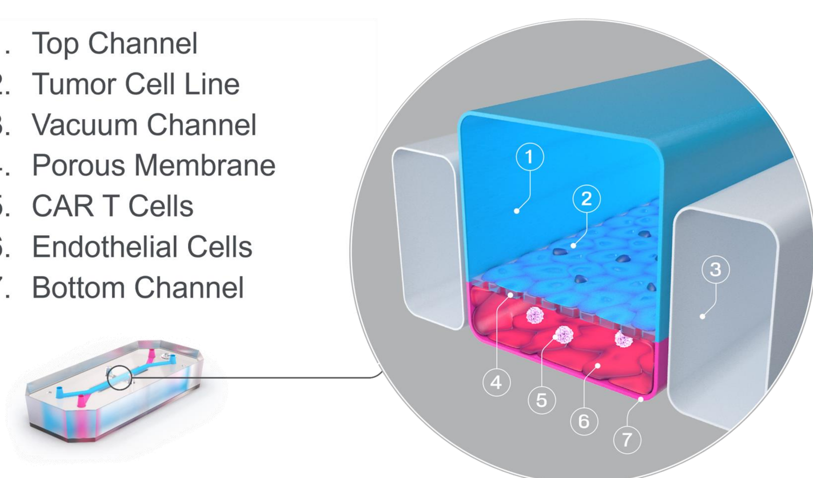

Figure 1. Schematic of the vascularized tumor cell line model. Chip-S1® Stretchable Chips from Emulate were seeded with a human HER2⁺ non-small cell lung cancer cell line (NSCLC, A549) in the top channel and tissue-matched lung microvascular endothelial cells (HMVEC-L) in the vascular (bottom) channel to create a tumor-vascular interface. Endpoint readouts can be performed via effluent cytokine analysis, confocal imaging, immune cell extraction and phenotyping by Flow Cytometry.

Modeling Solid Tumor CAR T-cell Recruitment and Effector Function On-Chip

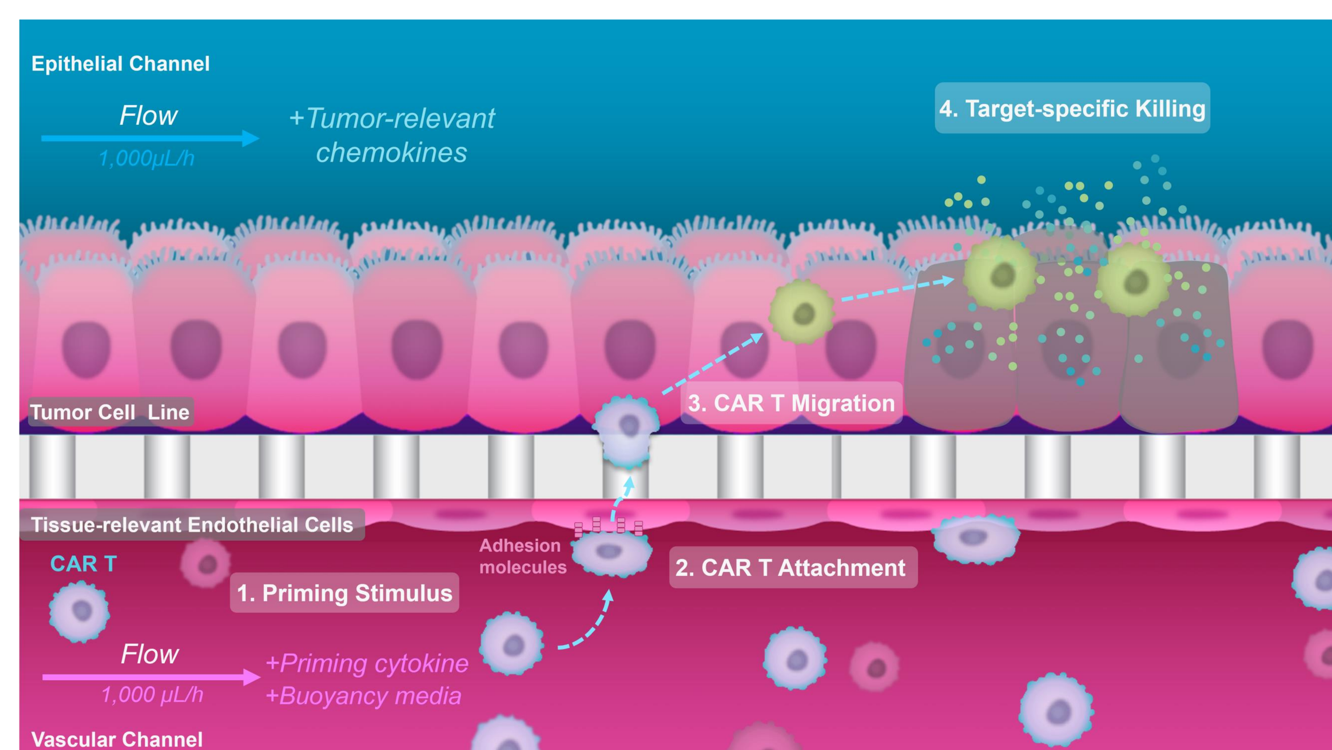

Figure 2. Lentiviral-transduced CAR T cells (4-1BB and CD3z signaling domains) were obtained from ProMab. HER2 CAR T cells and CD19 CAR T cells were used as the positive and negative controls, respectively. Pro-inflammatory 'priming' was used to allow circulating immune cells to attach to the vasculature and egress into tissues and tumors [1,2]. Starting on day 4 after cell seeding, 50 ng/mL TNF-α was administered to the vascular channel of NSCLC Organ-Chips to drive upregulation of endothelial cell adhesion molecules. Simultaneously, a NSCLC-specific cocktail of chemokines (100 ng/mL CXCL9, CXCL10, CCL2; 10 ng/mL CXCL11, Fractalkine) was administered in the epithelial channel to create a tumor-specific chemoattractant gradient [3-6]. After 24 h of chip priming, CAR T cells were labeled with CellTracker™ Red and perfused into the vascular channel for 4 h in 'buoyancy media', which maintains an even distribution of CAR T cells within the vascular channel at $1x10^6$ cells/mL. Perfusion was applied at a flow rate of 1,000 μL/h, which provides the biologically meaningful shear forces that normally impede immune cell attachment [1]. Following the 4 h CAR T cell perfusion, culture media without CAR T cells was flowed through the channels (at 30 μL/h) for 48 h to allow CAR T cell recruitment and killing responses to occur.

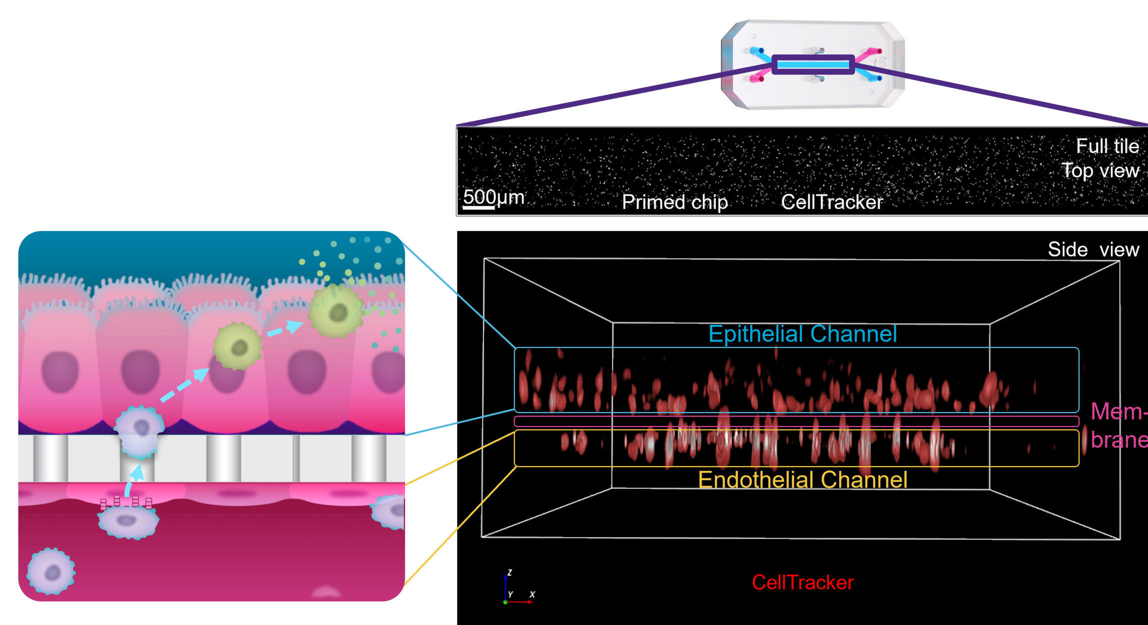

Figure 3. CAR T cell Recruitment to Top Channel and quantification. Prior to administration into the vascular channel, CAR T were labeled with CellTracker™ Red. Confocal z-stacks acquired post-fixation at 48 h demonstrates the ability to quantify CAR T cells at various stages of attachment and recruitment.

Validation of CAR T Killing of A549 Cells on Plates

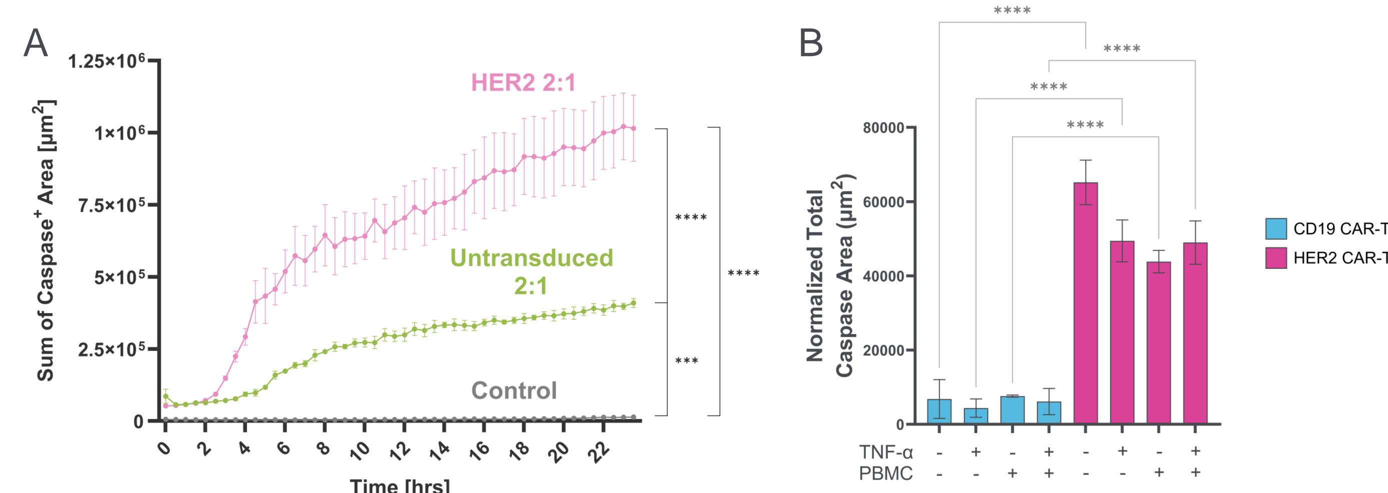

Figure 4. Antigen-specific efficacy of CAR T demonstrated through plate studies. **A)** A549 cells were administered with HER2 and un-transduced CAR T at a 2:1 (effector : target) ratio for 24 h. Live imaging demonstrated a significant increase in A549 killing (NucBlue 405) with HER2 CAR T compared to un-transduced T cells. **B)** A549 cells were administered with HER2 and CD19 CAR T at a 1:10 (effector : target) ratio for 24 h. HER2 CAR T showed antigen-specific caspase increase compared to CD19, which was not altered by the addition of peripheral blood mononuclear cells (PBMC) or cytokine treatment (TNFα, 50 ng/mL). Significance determined through One-way ANOVA with Tukey's multiple comparisons (***p<0.001,****p<0.0001); N=3 wells per condition; data shown as mean ± SEM.

CAR T Attachment and Migration On-Chip

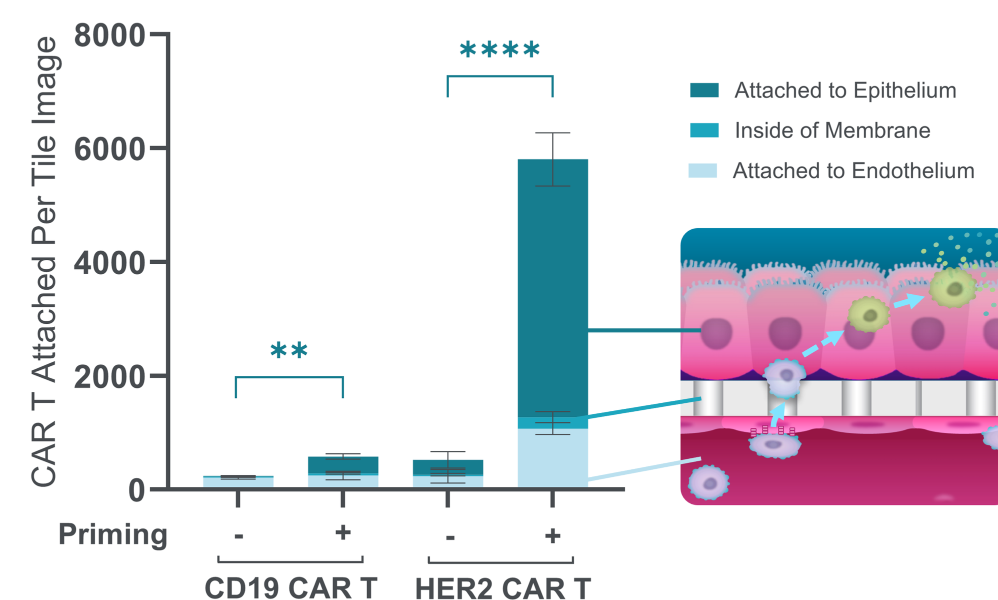

Figure 5. Cytokine priming-dependent migration into top epithelial channel. NSCLC Organ-Chips that were untreated or received cytokine priming were perfused with CAR T and fixed with paraformaldehyde after 48 h of flow. Quantification of confocal images demonstrates cytokine priming-dependent attachment and migration of CAR T. Interestingly, CD19 CAR T were found to have a significantly lower magnitude of attachment, potentially due to lack of antigen presence in top channel. Significance determined through unpaired T tests (**p<0.01,****p<0.0001); N=4 chips per condition; N=42 field of view per chip; data shown as mean ± SD.

CAR T Target Cell Killing and Caspase Response

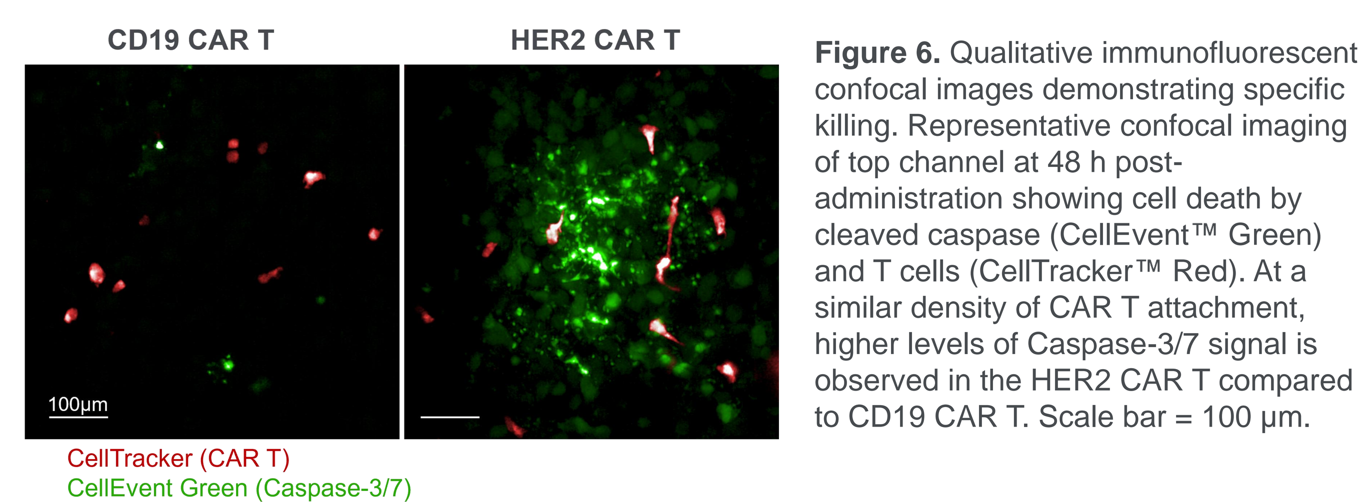

Figure 6. Qualitative immunofluorescent confocal images demonstrating specific killing. Representative confocal imaging of top channel at 48 h post-administration showing cell death by cleaved caspase (CellEvent™ Green) and T cells (CellTracker™ Red). At a similar density of CAR T attachment, higher levels of Caspase-3/7 signal is observed in the HER2 CAR T compared to CD19 CAR T. Scale bar = 100 μm.

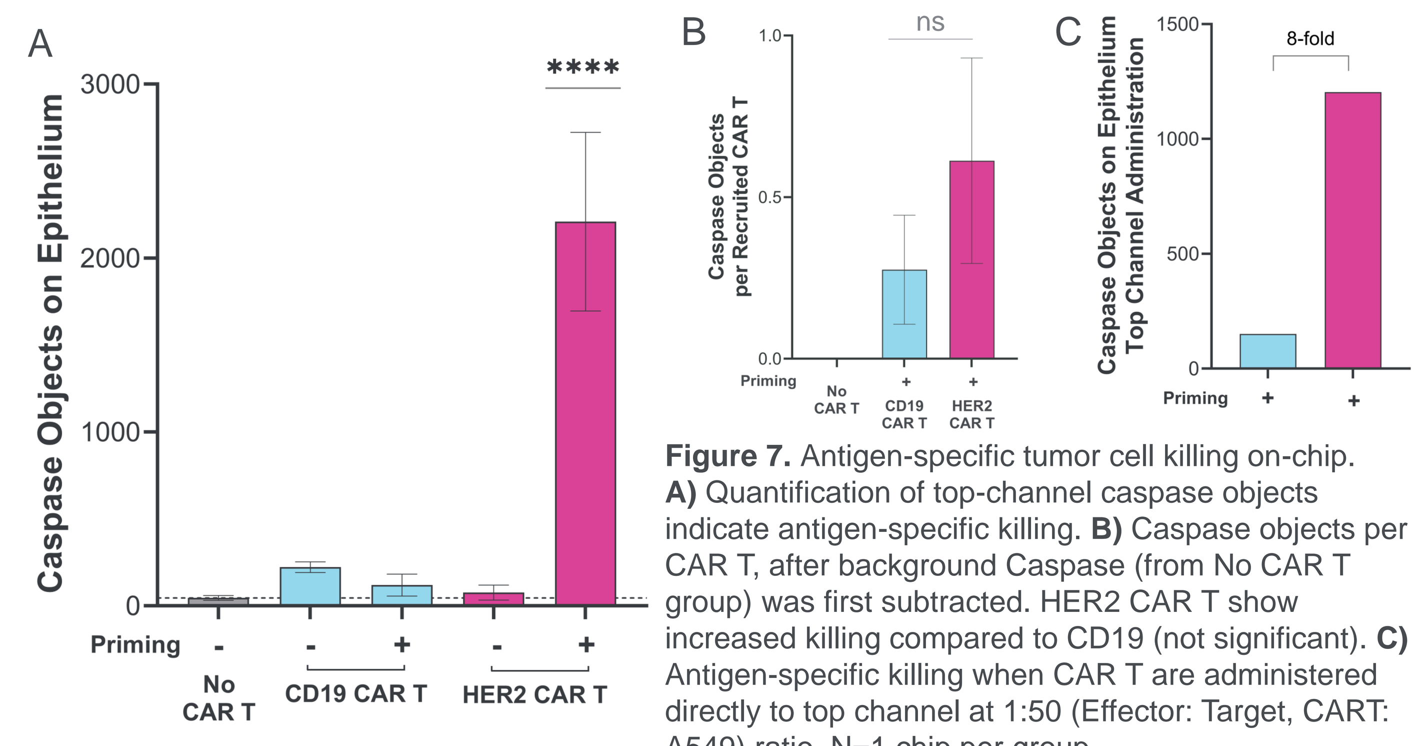

Figure 7. Antigen-specific tumor cell killing on-chip. **A)** Quantification of top-channel caspase objects indicate antigen-specific killing. **B)** Caspase objects per CAR T, after background Caspase (from No CAR T group) was first subtracted. HER2 CAR T show increased killing compared to CD19 (not significant). **C)** Antigen-specific killing when CAR T are administered directly to top channel at 1:50 (Effector: Target, CART: A549) ratio. N=1 chip per group.

Statistical significance determined by comparing all conditions to HER2 primed condition using ordinary one-way ANOVA with Tukey's multiple comparison test, ****p<0.0001, data shown as mean ± SD; N=4-7 chips per condition, N=42 field of view per chip.

Increased CAR T Fitness with Proof-of-Concept IL-2 Co-Therapeutic Treatment

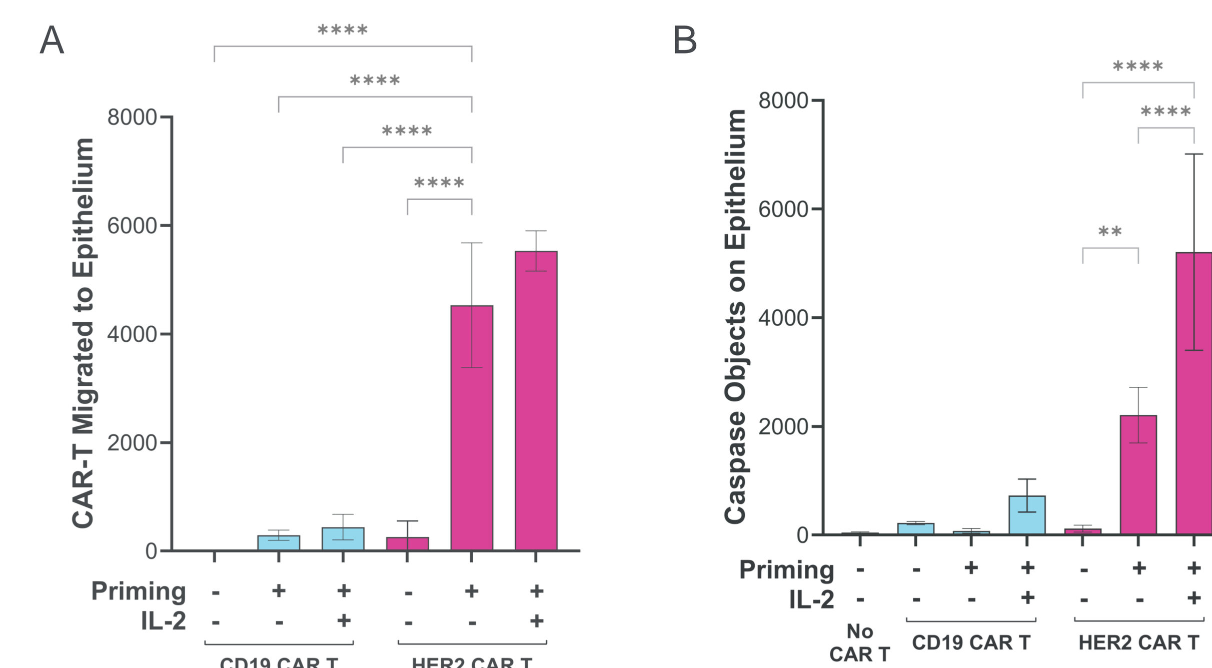

Figure 8. Proof-of-concept IL-2 co-therapy treatment demonstrated increased CAR T fitness. CAR T were pre-incubated for 4 h in media containing IL-2 [12.7 ng/mL], then co-administered with CAR T onto the Organ-Chips for 24 h. IL-2 was then removed from media for the final 24 h of flow. **A)** Increased recruitment to top channel and **B)** Significantly increased killing efficacy of CAR T was observed at 48 h with IL-2 treatment. Significance determined through One-way ANOVA with Tukey's multiple comparisons (**p<0.01,****p<0.0001); N=4-6 chips per condition; data shown as mean ± SD.

Cytokine Release from CAR T-cell Mediated Target Cell Killing

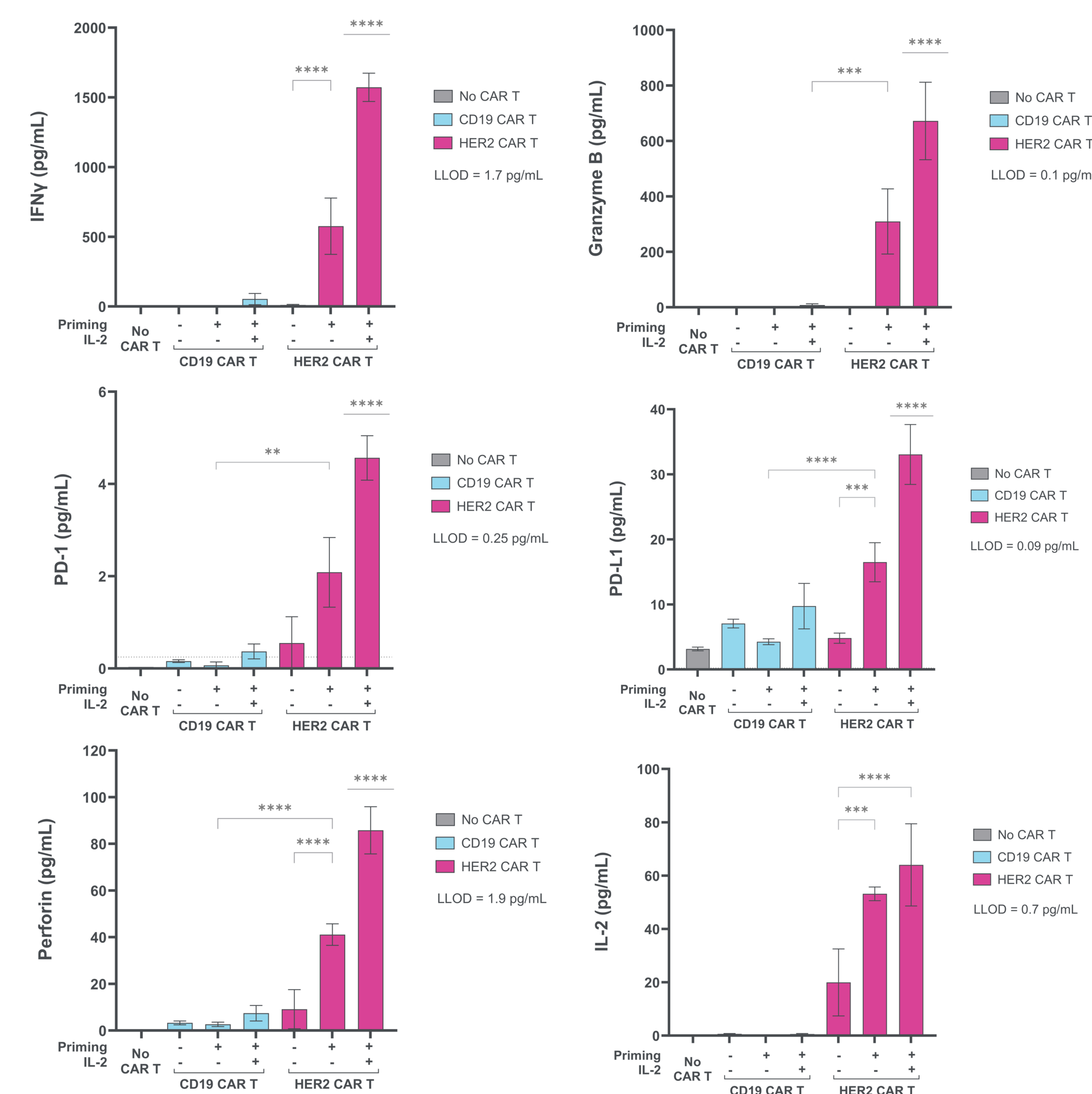

Figure 9. Antigen-specific release of soluble killing markers measured from top channel effluent at 48 h. Media was sampled from the top channel outlets every 24 h and analyzed using multiplex cytokine analysis (data shown here is from 48 h). Enhanced CAR T-cell killing response of HER2 CAR T (+ priming) and HER2 CAR T (+ priming + IL-2) was observed. Significance determined by one-way ANOVA with Tukey's multiple comparison test, **p<0.01, ***p<0.001, ****p<0.0001, data shown as mean ± SD, lower limit of detection (LLOD) of assay noted; N=4-6 chips per condition.

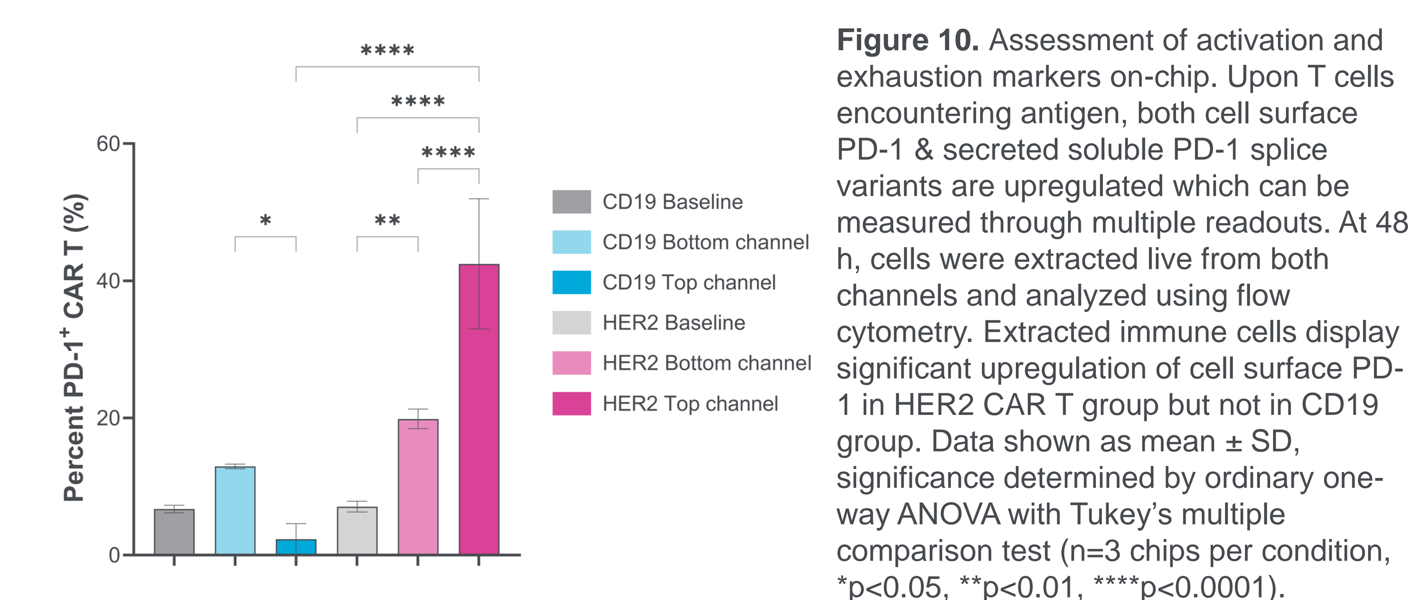

Figure 10. Assessment of activation and exhaustion markers on-chip. Upon T cells encountering antigen, both cell surface PD-1 & secreted soluble PD-1 splice variants are upregulated which can be measured through multiple readouts. At 48 h, cells were extracted live from both channels and analyzed using flow cytometry. Extracted immune cells display significant upregulation of cell surface PD-1 in HER2 CAR T group but not in CD19 group. Data shown as mean ± SD, significance determined by ordinary one-way ANOVA with Tukey's multiple comparison test (n=3 chips per condition, *p<0.05, **p<0.01, ****p<0.0001).

Conclusion

These findings suggest that this human-centric Organ-Chip model can evaluate the efficacy of CAR T cell therapies for solid tumors, providing a model that integrates the critical rate-step of CAR T recruitment along with killing.

References

[1] Getting to the site of inflammation: the leukocyte adhesion cascade updated. Ley, K., et al. 2007, Nature reviews. Immunology, 7(9), pp. 678–689. https://doi.org/10.1038/nri2156.
[2] T-cell function and migration. Two sides of the same coin. von Andrian, U. H. and Mackay, C. R. 2000, The New England journal of medicine, 343(14), pp. 1020–1034. https://doi.org/10.1056/NEJM200010053431407.
[3] Role of Cytokines and Chemokines in NSCLC Immune Navigation and Proliferation. Ramachandran, S., et al. 2021, Oxidative medicine and cellular longevity, 2021, pp. 1–20, https://doi.org/10.1155/2021/5563746.
[4] Role of Chemokines in Non-Small Cell Lung Cancer: Angiogenesis and Inflammation. Rivas-Fuentes, S., et al. 2015, Journal of Cancer, 6(10), pp. 938–952. https://doi.org/10.7150/jca.12286.
[5] Role of CXC group chemokines in lung cancer development and progression. Spaks, A. 2017, Journal of thoracic disease, 9(Suppl 3), pp. S164–S171. https://doi.org/10.21037/jtd.2017.03.61.
[6] Chemokines and NSCLC: Emerging role in prognosis, heterogeneity, and therapeutics. Srivastava, S., et al. 2022, Seminars in cancer biology, 86(Pt 2), pp. 233–246. https://doi.org/10.1016/j.semcancer.2022.06.010.

emulate

© 2024 Emulate, Inc | 27 Drydock Ave. 5th Floor | Boston, MA 02210